Published in final edited form as:
Sci Transl Med. 2011 September 21; 3(101): 101ra93. doi:10.1126/scitranslmed.3002214.

Teriparatide, a Chondro-Regenerative Therapy for Injury-Induced Osteoarthritis

Erik R. Sampson[1], **Matthew J. Hilton**[1], **Ye Tian**[1], **Di Chen**[1], **Edward M. Schwarz**[1], **Robert A. Mooney**[2], **Susan V. Bukata**[1], **Regis J. O'Keefe**[1], **Hani Awad**[3], **J. Edward Puzas**[1], **Randy N. Rosier**[1,†], and **Michael J. Zuscik**[1,†]

[1]Department of Orthopaedics & Rehabilitation, Center for Musculoskeletal Research, University of Rochester Medical Center, 601 Elmwood Avenue, Box 665, Rochester, NY, USA

[2]Department of Pathology & Laboratory Medicine, Center for Musculoskeletal Research, University of Rochester Medical Center, 601 Elmwood Avenue, Box 665, Rochester, NY, USA

[3]Department of Biomedical Engineering, Center for Musculoskeletal Research, University of Rochester Medical Center, 601 Elmwood Avenue, Box 665, Rochester, NY, USA

Abstract

There is no disease-modifying therapy for osteoarthritis, a degenerative joint disease that is projected to afflict more than 67 million individuals in the US alone by 2030. As disease pathogenesis is associated with inappropriate articular chondrocyte maturation resembling that seen during normal endochondral ossification, pathways that govern the maturation of these cells are candidate therapeutic targets. It is well established that parathyroid hormone (PTH) induces matrix synthesis and suppresses maturation of chondrocytes via the type 1 PTH receptor. We have found that the PTH receptor is up-regulated in articular chondrocytes following meniscal injury and during osteoarthritis in humans and in a mouse model of injury-induced knee osteoarthritis. Thus, we hypothesized that recombinant human PTH(1–34) (teriparatide) would inhibit aberrant chondrocyte maturation and associated articular cartilage degeneration. To test this, we administered systemic teriparatide (Forteo), an FDA-approved treatment for osteoporosis, either immediately after or 8 weeks after meniscal/ligamentous injury in mice. Knee joints were harvested at 4, 8, or 12 weeks post-injury to examine the effects of teriparatide on cartilage degeneration and articular chondrocyte maturation. Confirming successful systemic delivery of the drug, micro-computed tomography revealed increased bone volume within joints from teriparatide-treated mice compared to saline-treated controls. Immediate systemic administration of teriparatide increased proteoglycan content and inhibited articular cartilage degeneration, whereas delayed treatment beginning 8 weeks post-injury induced a regenerative effect. The chondro-protective and chondro-regenerative effects of teriparatide correlated with decreased levels of type × collagen, Runx2, matrix metalloproteinase-13 and the c-terminal aggrecan cleavage product NITEGE. These preclinical findings provide proof-of-concept that teriparatide (Forteo) may be useful for decelerating cartilage degeneration and inducing matrix regeneration in osteoarthritis patients.

Corresponding author erik_sampson@urmc.rochester.edu (E. R. S.).
†Both authors contributed equally to this work.

Author contributions: Study design and experimental planning: E.R.S., M.J.H., R.A.M., D.C., E.M.S., S.V.B., R.J.O., H.A., J.E.P., R.N.R., and M.J.Z. Execution of experiments and data collection: E.R.S., M.J.H., Y.T., R.N.R., and M.J.Z. Data analysis and interpretation: E.R.S., M.J.H., R.A.M., E.M.S., R.J.O., H.A., J.E.P., R.N.R., and M.J.Z. Preparation of the manuscript: E.R.S., R.N.R., and M.J.Z.

Competing interests: S.V.B. is a consultant for Eli Lilly; E.R.S., H.A., S.V.B., R.J.O., J.E.P., R.N.R. and M.J.Z. declare U.S. Provisional Patent Application No. 61/104,942 entitled "Protecting and repairing cartilage and musculoskeletal soft tissues" related to this work. The other authors declare no competing interests.

INTRODUCTION

Since 2005, arthritis has been ranked as the number one cause of disability in the United States [1]. In 2008, 27 million Americans were afflicted by osteoarthritis (OA) [2], with 25% of the adult US population (>67 million people) projected to have the disease by 2030 [3]. Although there are numerous established causes of OA, the disease process is always characterized by progressive articular cartilage degeneration, subchondral sclerosis, and osteophyte formation, which culminates in complete loss of cartilage and bone-on-bone articulation (eburnation) during end-stage disease [4–6]. Trauma that causes damage to the meniscus or ligaments within the knee is widely accepted as a common cause of OA in this joint [7], with an estimated 6-fold increase in the risk of developing radiographic evidence of disease within 21 years post-injury [8]. Current treatments for OA are palliative, aimed at reducing pain, which is the main symptom of the disease [9]. In advanced disease, the joint may be surgically replaced; however, this is a major surgical procedure with considerable morbidity as well as long-term consequences owing to joint failure and infection [9].

The articular chondrocyte is the cell responsible for maintenance of articular cartilage in adults [10]. As opposed to chondrocytes associated with bone development and growth, articular chondrocytes do not normally undergo hypertrophic maturation leading to matrix mineralization. Instead, they persist in their expression of collagen types II, VI, IX, and XI, cartilage oligomeric matrix protein and aggrecan, all of which are secreted proteins essential for the integrity of articular cartilage [11]. In the context of OA, articular chondrocytes begin expressing genes associated with maturation during endochondral ossification, including type × collagen, alkaline phosphatase and Runx2. Catabolic enzymes, including matrix metalloproteinases 9 and 13 (MMP9 and MMP13) and a disintegrin and metalloproteinase with thrombospondin motifs 4 and 5 (ADAMTS4 and ADAMTS5), are also up-regulated [11–15]. Biochemical, genetic, and mechanical factors are likely contributors to this change in cell phenotype, which culminates with degeneration of cartilage in OA. Thus, strategies to inhibit aberrant hypertrophic maturation and to induce matrix production in articular chondrocytes could represent potential new therapeutic modalities.

There is an abundance of literature documenting the stimulatory effects of parathyroid hormone (PTH) on bone formation [16–18]. This work led to the development of Forteo (Eli Lilly), the FDA-approved formulation of recombinant human PTH(1–34) (teriparatide), which is a bone anabolic therapy for osteoporosis [19]. Although the mechanism underlying the anabolic action of teriparatide treatment on bone is not fully understood, direct effects on osteoblast proliferation and survival are likely important [16, 20, 21]. In addition to bone as a target, signaling downstream of the type I parathyroid hormone receptor (PTHR1) regulates chondrocyte differentiation [22, 23]. Parathyroid hormone-related peptide (PTHrP), another PTHR1 ligand, is a potent stimulator of proliferation and matrix synthesis and suppressor of maturation [24, 25]. Mice that are homozygous for the ablation of *Pthrp* [26] or *Pthr1* [27] display accelerated chondrocyte maturation and premature bone formation. Conversely, animals over-expressing PTHrP in the growth plate display delayed terminal differentiation and a disruption of normal mineral deposition [28]. Chondrocyte-targeted over-expression of the constitutively active PTHR1 mutant that causes Jansen's metaphyseal chondrodysplasia also induces disorganization of the growth plate with delayed terminal differentiation [29]. These *in vivo* data [reviewed in [30, 31]] collectively implicate PTHR1 signaling as a key regulator of chondrocyte differentiation and endochondral ossification.

PTHrP is normally expressed by articular chondrocytes in low amounts and is increased following application of mechanical load [32, 33] or in OA [34]. It has been established recently that PTHrP is required for articular cartilage maintenance given that *Gdf5-Cre*-targeted knockdown of PTHrP in mid-region articular chondrocytes leads to accelerated development of posttraumatic OA in the mouse [35]. Along with data presented in this report, there is also evidence that PTHR1 is up-regulated in osteoarthritic cartilage [36]. Given the proliferative and matrix anabolic effects of PTHR1 signaling in chondrocytes and the requirement for PTHrP in the maintenance of articular cartilage, the up-regulation of PTHR1 in articular chondrocytes during OA might represent an endogenous attempt at repair. Based on this, we designed experiments to test the hypothesis that teriparatide may have therapeutic potential for treating OA. To test this hypothesis, we examined the ability of systemic, intermittent teriparatide treatment to decelerate cartilage degeneration, inhibit AC maturation, and stimulate matrix synthesis in an established mouse meniscal/ligamentous injury (MLI) model of knee OA [37, 38].

RESULTS

PTHR1 is up-regulated in OA cartilage and following meniscal injury

To examine PTHR1 expression in articular chondrocytes following meniscal injury or in progressive OA in humans, and following MLI in mice, protein and mRNA levels were examined using immunohistochemistry and qPCR, respectively. Normal human articular cartilage was obtained from amputation patients and injured cartilage was obtained from patients undergoing arthroscopic treatment of meniscal injuries that involved articular cartilage debridement. Representative immunohistochemistry revealed that although PTHR1 was not detectable in articular chondrocytes in normal cartilage (Fig. 1A), cellular expression of PTHR1 was observed in cartilage from human patients with meniscal injury (Fig. 1B) or with progressive OA (Fig. 1C). The expression pattern was similar in the mouse, with increased PTHR1 expression in articular chondrocytes from MLI joints (Fig. 1E; red arrows) compared to sham-operated joints (Fig. 1D). As expected, osteoblasts and osteocytes in the subchondral bone were PTHR1-positive in both control and MLI joints (Fig. 1D and 1E, black arrows). Consistent with this, qPCR analysis of mRNA harvested from articular cartilage revealed that *Pthr1* mRNA expression was 5-fold greater in MLI versus sham joints (Fig. 1F, $P < 0.05$). *Mmp13* and *Adamts5*, transcripts for enzymes responsible for the degradation of type II collagen and proteoglycans, respectively, were also up-regulated in injured joints compared to controls (Fig. 1F), confirming a progressive degenerative process following MLI. These results establish that PTHR1 is increased in both human and mouse articular cartilage following meniscal injury and in progressive human OA, priming articular chondrocytes to be responsive to endogenous PTHrP as a repair response. In this context, PTHR1 might represent a therapeutic target for systemically delivered exogenous teriparatide.

Systemic administration of Forteo has anabolic effects on bone

The bone anabolic effect of teriparatide was confirmed using microCT analysis and detection of *type I collagen* (*Col1a1*) expression via *in situ* hybridization. Sham-operated and MLI mice were administered either saline or Forteo (40 μg/kg/day), commencing after MLI surgery (immediate) or 8 weeks later (delayed). Forteo treatment lasted either 12 weeks for the ‘immediate’ group or 4 weeks for the ‘delayed’ group. In sham-operated mice, bone volume was greater in Forteo-treated mice compared to saline-treated controls (Fig. 2A, immediate and delayed), confirming that both administration regimens induce a bone anabolic effect similar to that published [16]. In injured mice, there was an increase in bone volume in both the saline-treated groups (Fig. 2B, immediate and delayed) compared to saline-treated, sham-operated controls (Fig. 2A, immediate and delayed), which is consistent

with the development of a sclerosis in the subchondral plate that is associated with the OA degenerative process seen in humans [39]. In MLI mice, both immediate and delayed treatment of MLI mice with teriparatide increased bone volume significantly compared to the saline-treated MLI groups (Fig. 2B, $P < 0.05$). This increased bone volume with delayed teriparatide treatment in MLI mice was associated with increased expression of *Col1a1* by cells in the subchondral bone (Fig. 2C and D), further confirming the bone anabolic effects of systemic teriparatide treatment in the joint region.

Forteo increases JAGGED1 expression in articular chondrocytes following MLI

JAGGED1 (JAG1) immunohistochemistry was performed to confirm that systemic administration of teriparatide leads to cartilage-specific responses in injured joints. JAG1, a membrane-bound ligand in the Notch signaling pathway, was chosen as a readout of receptor activation because of its direct transcriptional activation in response to PTHR1 signaling in several cell types, including osteoblasts and periodontal ligament cells [40]. Beginning 8 weeks after MLI surgery (delayed administration), mice were treated with either saline or Forteo for 4 weeks, and joints were harvested. Joints from Forteo-treated MLI mice showed a greater amount of articular chondrocyte JAG1 immunoreactivity (Fig. 2F, red arrows) compared to saline-treated controls (Fig. 2E), establishing that the systemic, intermittent treatment regimen delivers Forteo to the joint where it can exert a direct effect on articular chondrocytes.

Teriparatide enhances proteoglycan content during early degeneration in MLI joints

To determine whether teriparatide induction of PTHR1 signaling in articular chondrocytes influences the progression of injury-induced cartilage degeneration, mice administered sham surgery or MLI were treated immediately with saline, Forteo or PTH, and joints were harvested 4 weeks later. Histomorphometry was performed to quantify cartilage area and Alcian Blue staining was employed to assess proteoglycan content in the articular cartilage. At this early time point, histological analysis revealed only mild arthritic changes in injured joints, notably fibrillation (Fig. S1D, S1E and S1F, black arrows). No difference in articular cartilage area in sham versus injured joints was discernable by quantitative histomorphometry (Fig. S1G). The up-regulation of PTHR1 mRNA and protein 8 weeks following MLI (Fig. 1) suggested that articular chondrocytes acquired sensitivity to teriparatide prior to substantial articular cartilage degeneration. Although neither Forteo nor PTH treatment affected articular cartilage area in injured joints at this early time point, there was increased articular cartilage Alcian Blue staining intensity in treated mice (Fig. S1G), suggesting that teriparatide induces proteoglycan synthesis in articular chondrocytes in cartilage that is beginning to undergo injury-induced osteoarthritic degeneration. There was no apparent difference in articular cartilage Alcian Blue staining intensity in sham-operated joints in mice treated with saline versus Forteo or PTH (Fig. S1A–S1C), which confirms that teriparatide only stimulates proteoglycan matrix production in articular chondrocytes with increased PTHR1 following meniscal/ligamentous injury.

Immediate treatment with Forteo inhibits articular cartilage loss following MLI

By 12 weeks after surgery in saline-treated mice, there was extensive articular cartilage degeneration in MLI joints (Fig. 3C) compared to sham-operated joints (Fig. 3A). Comparatively, while immediate treatment of sham-operated mice with Forteo did not alter cartilage morphology (Fig. 3B), it decelerated cartilage degeneration in MLI joints (Fig. 3D). Mouse OARSI scoring of joint cartilage revealed a significantly better score in injured joints of mice administered Forteo than in saline-treated controls (Fig. 3E). Moreover, histomorphometric analysis of MLI joints revealed that Forteo treatment inhibited the OA-like decrease in articular cartilage area between the 8 and 12 week time points seen in saline-treated mice, evidenced by 27% more articular cartilage area following Forteo versus

saline treatment 12 weeks post-injury (Fig. 3F, $P < 0.05$). These results establish that immediate systemic treatment with teriparatide following MLI in mice is chondro-protective, supporting it as a candidate therapeutic agent that can suppress cartilage loss in OA, which is the central hallmark of the degenerative process in human disease.

Delayed treatment with Forteo induces articular cartilage regeneration following injury

To examine the effect of Forteo on cartilage that is progressively degenerating, a 4-week treatment period with saline or Forteo was initiated 8 weeks after sham surgery or MLI. This delayed regimen was employed to examine the impact of treatment in the context of the clinically relevant situation where the therapy would be initiated after a diagnosis of OA during the progressive degeneration stage. Representative histological sections from joints 12 weeks after injury surgery (4 weeks after initiation of treatment) showed that saline-treated MLI mice displayed substantial cartilage loss that involved exposure of the subchondral bone in some areas (Fig. 4C), which is in contrast to the intact articular cartilage layer seen in sham-operated joints (Fig. 4A). Forteo-treated MLI mice (Fig. 4D) displayed a larger amount of cartilage than saline-treated MLI mice (Fig. 4C)—a finding that was consistent with the effect of immediate teriparatide treatment seen in Fig. 3. Mouse OARSI scoring of the joints supported these histological results, with significantly lower scoring of the Forteo-treated MLI joints compared to the saline-treated control group (Fig. 4E, $P < 0.05$).

To investigate whether teriparatide induces cartilage matrix production, Alcian Blue stain in histological sections was quantified to evaluate proteoglycan content. Image analysis revealed a nearly 3-fold increase in Alcian Blue stained matrix in delayed Forteo-treated MLI joints compared to the saline-treated MLI controls (Fig. 4F, $P < 0.05$). This was consistent with the effect of teriparatide at 4 weeks after MLI when administered immediately, where a >3-fold increase in proteoglycan staining was also observed (fig. S1). Histomorphometric analysis of cartilage area supported this by establishing that the delayed Forteo-treated groups had significantly more cartilage than both saline-treated mice at 12 weeks after MLI (32% increase) and saline-treated mice at 8 weeks after MLI (21% increase) (Fig. 4G, $P < 0.05$). Overall, the increased proteoglycan matrix staining and increased cartilage area compared to that seen at 8 weeks after MLI suggests that systemic Forteo treatment has a chondro-regenerative effect in degenerating cartilage.

To establish that the observed effects of Forteo are not specific to the clinical Forteo formulation that was administered to the injured mice, we repeated this experiment using recombinant human PTH(1–34). As done previously with Forteo, a 4-week treatment period with saline or PTH was initiated 8 weeks following administration of sham surgery or MLI. Representative histologic sections from joints 12 weeks after surgery (4 weeks after initiation of treatment) showed the expected degeneration following MLI (Fig. S2A, S2C), with PTH-treated mice (Fig. S2D) displaying a larger amount of cartilage than saline-treated mice (Fig. S2C). Mouse OARSI scoring of the joints supported this observation, with significantly lower scores for PTH-treated MLI joints compared to the saline-treated control group (Fig. S2E). Imaging to quantify proteoglycan content revealed nearly 3-fold more Alcian Blue-stained matrix in PTH-treated MLI joints compared to saline-treated MLI control joints (Fig. S2F). Finally, histomorphometric analysis of cartilage area established that the PTH-treated groups had significantly more cartilage than both saline-treated mice at 12 weeks post-MLI (24% increase, Fig. S2G) and saline-treated mice at 8 weeks post-MLI (13%, Fig. S2G, blue bar and red line). These results establish generic recombinant human parathyroid hormone (1–34) induces the same chondro-regenerative effect as Forteo.

Finally, the observed chondro-regenerative effect of delayed Forteo administration correlated with increased expression of *Proteoglycan4* (*Prg4*) mRNA by articular

chondrocytes in MLI joints as determined by *in situ* hybridization. In a representative section from a sham-operated joint (Fig. 5A), *Prg4*, whose gene product is necessary for proper joint lubrication and function [41, 42], was expressed in the articular cartilage (red arrows) and posterior medial meniscus (blue arrows). *Prg4* expression was lost in articular chondrocytes in MLI joints from saline-treated mice, although expression in the non-surgically manipulated posterior medial meniscus was maintained (Fig. 5B, blue arrows). Delayed Forteo treatment restored the expression of *Prg4* in articular chondrocytes in degenerating cartilage (Fig. 5C, red arrows), providing further evidence of a chondro-regeneration. Notably, Forteo did not increase the expression of *Prg4* in the meniscus (Fig. 5B and C, blue arrows), indicating a selective effect of the therapy in degenerating cartilage that is populated by PTHR1-expressing articular chondrocytes (Fig. 1). Overall, teriparatide induces a chondro-regenerative effect as evidenced by increased synthesis of critical matrix components, including *Prg4*, in degenerating cartilage. These results further establish a clinically relevant therapeutic potential for this agent in treating progressive OA.

Forteo treatment inhibits articular chondrocyte maturation and cartilage matrix degradation

It is hypothesized that OA pathophysiology stems, in part, from inappropriate endochondral ossification-like articular chondrocyte maturation [15, 43]. Therefore, effective therapeutic strategies should aim to inhibit this aberrant maturation. We examined the expression of type × collagen (COL10a1) and RUNX2 in normal and arthritic joints harvested from mice administered saline or Forteo following MLI or sham surgery. Suggesting that injury-induced degeneration is associated with maturation of articular chondrocytes, MLI joints displayed enhanced COL10a1 levels (Fig. 6B) and increased cellular expression of RUNX2 (Fig. 6E, red arrows) compared to sham operated joints (Fig. 6A and 6D, respectively). Regarding the COL10a1 expression pattern, it was mainly restricted to the most hypertrophic cells in the deep layers of the cartilage in the sham-operated, saline-treated group (Fig. 6A, red arrows); whereas the more robust cellular and matrix staining in the arthritic joints was located near the cartilage surface (Fig. 6B, red and blue arrows, respectively). Consistent with the known inhibitory effect of PTHR1 activation on chondrocyte maturation [22–25], injured joints from mice treated with Forteo showed significantly reduced cellular and matrix COL10a1 levels in the non-calcified articular cartilage (Fig. 6C) as well as reduced cellular expression of RUNX2 (Fig. 6F), compared to saline treatment (Fig. 6B and 6E, respectively).

In addition to inhibiting the expression of genes associated with chondrocyte maturation, Forteo reduced the degradation of matrix in joints post-MLI. Consistent with mRNA results presented in Fig. 1F, protein levels of the catabolic enzyme MMP13 were increased in injured joints from saline-treated mice (Fig. 6H, red arrows) relative to sham-operated joints (Fig. 6G). In MLI joints from mice treated with Forteo (Fig. 6I), MMP13 levels were reduced compared to the saline-treated group (Fig. 6H). Regarding proteoglycan degradation, immunostaining for the c-terminal aggrecan cleavage product NITEGE revealed the expected increase in aggrecan matrix degradation in MLI joints (Fig. 6K) compared to sham-operated control joints (Fig. 6J). Red arrows denote enhanced cellular NITEGE staining in the meniscus (M) and tibial plateau articular cartilage (T) and blue arrows identify areas of cartilage matrix with enhanced NITEGE staining. Suggesting inhibition of aggrecan breakdown in Forteo-treated MLI mice, NITEGE staining was reduced (Fig. 6L) compared to saline-treated MLI mice (Fig. 6K). These results establish that systemically administered Forteo reduces MMP13 levels and inhibits aggrecan degradation, suggesting the potential efficacy of teriparatide-based therapy in the inhibition of matrix catabolism that is central to the tissue phenotype present in the context of injury-induced OA.

Teriparatide treatment does not enhance osteophyte formation

A key feature of human OA is the development of osteophytes in the joint margins [39]. Since PTHR1 signaling induced by Forteo leads to bone anabolic effects (Fig. 2A and 2B), we examined whether MLI-induced osteophyte formation was exacerbated in MLI mice treated with either Forteo or PTH. Three dimensional reconstructions were generated from the same microCT data sets that were collected for the morphometric data (Fig. 2A and 2B). As depicted in the representative reconstructions, sham-operated mice treated with saline or Forteo did not display any sites of ectopic bone formation reminiscent of osteophytes at 12 weeks post-surgery (Fig. S3A and S3B). As expected, MLI joints from mice treated with saline for 12 weeks showed significant mineral deposition at the joint margins and had enhanced mineralization of the meniscus (Fig. S3C). Interestingly, Forteo treated mice did not show enhanced osteophyte formation in the injured joints (Fig. S3D) compared to the saline-treated control mice (Fig. S3C). This finding was confirmed by histologic assessment of osteophyte number and mean diameter at the anterior and posterior margins of the tibial plateau. Images from representative sham-operated or MLI joints from mice given delayed saline or Forteo indicate that no osteophytes were initiated in sham-operated joints regardless of treatment (Fig. S3E and S3F). Comparatively, representative histology of MLI joints from mice treated with either saline or Forteo did reveal osteophytes in the anterior aspect of the medial compartment (Fig. S3G and S3H, blue arrows). Furthermore, neither Forteo nor PTH treatment caused an increase osteophyte number or diameter (Fig. S3I and S3J), with Forteo actually reducing osteophyte mean diameter in MLI joints from mice treated using the delayed regimen (Fig. S3J). Overall, these results suggest that teriparatide therapy does not induce or exacerbate osteophyte formation that is naturally initiated by the degenerative process in this model.

DISCUSSION

The most routinely recommended treatments for OA, including orally administered or locally injected anti-inflammatory agents and analgesics, are palliative, with surgical joint replacement the only option in advanced disease [9]. The only therapies purported to be disease-modifying aim to replenish cartilage proteoglycan components via dietary supplementation with chondroitin sulfate/glucosamine [44, 45] or via intra-articular injection of hyaluronic acid (e.g. Synvisc) [46, 47]. However, there is no consensus on the efficacy of oral ingestion of aggrecan sugar moieties [45], and joint injections of hyaluronic acid demonstrate efficacy at relieving knee joint pain, but only for brief periods of up to 6 months [47]. Therefore, the development of an effective agent supporting protective and/or regenerative effects in articular cartilage would have an immediate and major impact on standard of care for this pervasive and debilitating disease. Our findings establish teriparatide, in particular the FDA-approved drug Forteo, as a disease-modifying candidate therapeutic that has both chondro-protective and chondro-regenerative capabilities in the context of OA.

At a cellular level, it has been suggested that aberrant maturation of articular chondrocytes along a pathway that resembles endochondral ossification contributes to OA progression [15, 43]. This inappropriate articular chondrocyte differentiation is associated with the up-regulation of Runx2 [48], type × collagen [12, 13], and MMP13 [43, 49], as well as increased apoptosis [14] and other hallmarks of chondrocyte maturation [15], in both human OA and animal models of disease. Consistent with this, in our mouse model of MLI-induced OA, we observed the up-regulation of *Adamts5*, COL10a1, RUNX2, MMP13 message and protein and increased degradation of aggrecan in degenerating articular cartilage.

Signaling pathways inducing chondrocyte maturation and OA-like cartilage degeneration include loss of TGF-β signaling in mice [50–52]; gain of WNT/β-CATENIN signaling in

mice [53, 54] and humans [55–57]; gain of Indian Hedgehog (IHH) signaling in mice and humans [58]; and increased HIF2α expression leading to enhanced IHH/RUNX2 signaling in mice [59, 60]. These pro-maturation shifts in articular chondrocyte signaling are generally consistent with the additional findings that RUNX2 is up-regulated in injury-induced murine knee OA [48], and over-expression of RUNX2 in articular chondrocytes that are experiencing mechanical stress contributes to the pathogenesis of OA [61]. These and other similar findings implicate maturation-driving signals in the pathogenesis of OA.

Modulation of signaling pathways that activate chondrocyte maturation might be protective against cartilage degeneration. For example, *Runx2*-haploinsufficient mice administered a meniscal injury display less severe knee OA [48]. Similarly, pharmacologic and genetic inhibition of IHH signaling in mice protects against injury-induced degeneration of knee cartilage that is concomitant with down-regulation of *Runx2* and *ADAMTS5* [58]. Furthermore, inhibition of cartilage-degrading enzymes associated with chondrocyte maturation, such as MMP13 and ADAMTS5, has been underscored as the best current strategic direction for developing an OA therapeutic [62]. Thus, inhibition of inappropriate articular chondrocyte maturation and/or blockade of the associated matrix-degrading enzymes represent obvious targets for developing a treatment for OA.

It is well-established that parathyroid hormone and PTHrP are potent inhibitors of chondrocyte maturation [22, 23]. Specifically, activation of PTHR1 potently induces chondrocyte proliferation and matrix production (type II collagen and proteoglycans) while suppressing maturation [23–25]. This concept is supported by *in vitro* and *in vivo* data, where gain or loss of PTHR1 signaling respectively inhibits or accelerates chondrocyte hypertrophy [30, 31]. Owing to selective up-regulation of PTHR1, which we identified in human cartilage following meniscal injury or in progressive OA and in mouse cartilage following MLI, PTHR1 signaling may be protective and possibly even regenerative in the context of cartilage degeneration. This idea is supported by two studies which demonstrate that when administered intermittently via intra-articular injection, PTH can decelerate papain-induced cartilage degeneration in the rat [63] and can induce cartilage regeneration in a full-thickness osteochondral injury in the rabbit [64]. Although these studies suggest that PTH has chondro-regenerative potential, the models of cartilage degeneration and injury that were employed do not examine the effect of PTH during the OA disease process. Additionally, the daily intra-articular injection treatment regimen used in these studies is not clinically practical or translational, leaving open the need to examine the efficacy of the systemic mode of delivery that is currently FDA-approved for teriparatide. Therefore, the rationale for the present investigation of teriparatide as a potential systemic OA therapy was based on two key concepts: The broad literature, which establishes PTHR1 signaling in chondrocytes as an inducer of matrix production and inhibitor of maturation, and the selective up-regulation of PTHR1 after injury and in arthritic cartilage, which primes the cells to be targeted by teriparatide therapy.

The experimental design to test teriparatide as an OA therapy involved treatment of mice administered a meniscal/ligamentous knee injury followed by treatment with either Forteo or PTH at the 40 μg/kg/day dose. This dose was selected based on literature establishing that the effective teriparatide dose range for treatment of bone loss or fracture repair in mice is between 30 μg/kg/day and 400 μg/kg/day [16, 65–68]. In two of these studies, 40 μg/kg/day was demonstrated to effectively accelerate fracture healing in the mouse, with enhancement of chondrogenesis and expansion of the cartilaginous callus [65, 66]. It should be noted that 40μg/kg/day is significantly higher than accepted and optimal ranges in other species including rat (4–20μg/kg/day) [69, 70], rabbit (10 μg/kg/day) [71], macaque (5 μg/kg/day) [72], and human (0.25 μg/kg/day) [73]. We anticipate that there is a similar species-

associated shift in the range of effective concentrations supporting chondro-protective and chondro-regenerative effects.

Compared to saline treatment and when delivered immediately following injury, Forteo was chondro-protective, characterized by enhanced proteoglycan production by 4 weeks and decelerated cartilage degeneration at 12 weeks. Notably, the more clinically-relevant delayed treatment regimen elicited a chondro-regenerative and maturation-inhibiting effect, characterized by increased proteoglycan content in the articular cartilage, up-regulation of *Prg4*, an increased amount of articular cartilage, and decreased articular chondrocyte expression of COLXa1, RUNX2, and MMP13. Degeneration of aggrecan was also reduced. Chondro-regenerative effects were also observed when injured mice were treated with PTH, excluding the possibility that the effects are unique to the Forteo formulation. Ameliorating the concern that teriparatide might exacerbate osteophyte formation in degenerating joints, microCT analyses and histological measurement of osteophyte number and diameter establish that osteophytes were not increased in injured joints from Forteo-treated mice.

Histological and histomorphometric data suggest that inhibition of matrix-degrading enzymes may be more effective then teriparatide therapy at stopping degeneration of cartilage matrix during OA (74, 75). Specifically, compared to joints from injured mice treated with Forteo or PTH in the present study, the articular cartilage is better preserved following injury-induction of OA in *Adamts5* [74] and *Mmp13* [75] knockout mice. However, the genetic ablation of catabolic enzymes in these studies leads to complete arrest of matrix degeneration without affecting other changes associated with disease, including aberrant chondrocyte maturation, osteophyte formation and subchondral sclerosis. This is in contrast to the chondro-regeneration and inhibition of chondrocyte maturation seen in the present study following teriparatide administration, which suggests this therapy may be effective at decelerating several key disease phenotypes in addition to cartilage degeneration. Nevertheless, the chondro-preservation observed in the *Adamts5* and *Mmp13* knockout mice has led to the conclusion that inhibitory agents targeting these enzymes have remarkable therapeutic potential [62]. Initial studies in the rat have substantiated the *in vivo* efficacy of an aggrecanase inhibitor in the blockade of aggrecan degradation [76] and MMP inhibitors in decelerating cartilage degeneration [77, 78]. The only way to elicit similar cartilage preservation clinically would be to administer enzyme inhibitors before degeneration begins, and to persist with the treatment over the span of a lifetime. To begin treatment when a patient presents to the clinic with pain due to progressed disease would potentially prevent further degeneration, but it would not have a reparative effect that would build back matrix. A potential strategy for more effective therapeutic results would be to combine periodic teriparatide treatment with the administration of an ADAMTS or MMP inhibitor; this could lead to even more robust chondro-regeneration by teriparatide owing to the complementary blockade of matrix degradation.

Although teriparatide elicits a bone anabolic effect in the subchondral plate via activation of osteoblasts, it might simultaneously restrict the endochondral ossification-like process occurring in MLI-associated osteophytes. This would occur via inhibition of chondrocyte maturation in a manner analogous to the action of PTHrP in the developing growth plate. This possibility is supported by our findings that Forteo inhibits expression of genes associated with chondrocyte maturation in degenerating cartilage. Regarding the increased bone volume in the subchondral plate in both MLI and sham-operated joints following Forteo treatment, there is the concern that this effect might enhance subchondral sclerosis and exacerbate, rather than decelerate, the cartilage degeneration that occurs in clinical OA. This concern, coupled with practical considerations regarding the persistence of the chondro-protective or -regenerative effects of teriparatide after the treatment is stopped, represent key questions to be addressed.

There is evidence for teriparatide induction of osteosarcoma in rats administered long term daily treatment out to 2 years, with a 20–40% incidence at 70–80% of life span [79]. In our examination of articular cartilage in samples harvested from teriparatide-treated mice, we never observed a lesion consistent with a malignancy in the tibial or femoral metaphyses. Because these lesions are among the most common sites for primary osteosarcoma, we do not believe that our immediate or delayed treatment regimens are carcinogenic in the mouse. This is consistent with what has been reported in macaques, where teriparatide did not induce any osteosarcomas following long term treatment with 5 μg/kg/day [72]. Furthermore, human data suggest only 2 cases in >430,000 osteoporosis patients treated with Forteo developed osteosarcoma [73]. Thus, we believe that the increase in osteosarcoma incidence in teriparatide-treated rats probably is not prognostic of an equivalent risk in humans [80], and is possibly species-specific.

In conclusion, we have identified teriparatide as a novel candidate therapy for injury-induced OA that is both chondro-protective and chondro-regenerative. This impacts the arthritis field by providing the basis for FDA-approved Forteo as a disease-modifying therapy for OA with clinical potential. Overall, given the scope of the clinical problem and the current availability of Forteo for clinical use, our experimental findings make a compelling case for further characterization of this drug in a clinical trial aimed at evaluating its efficacy as a treatment for human OA.

MATERIALS AND METHODS

Procurement and fixation of human tissues

An Institutional Review Board-approved protocol was executed to collect discarded cartilage from patients undergoing orthopaedic surgery. Normal cartilage was collected from amputation patients (talus or knee, n=2), damaged cartilage was debrided from patients that underwent arthroscopic surgery to treat a meniscal injury (n=18), and OA cartilage was harvested from patients that underwent total knee arthroplasty (n=22). Tissues were fixed for 2 to 10 days in 10% neutral buffered formalin at 25°C. Samples were decalcified for 3 weeks in 10% w/v EDTA and then embedded in paraffin. Sections (3 μm) were cut and mounted on positively charged slides, baked at 60°C for 30 minutes, deparaffinized in xylene, and rehydrated in decreasing concentrations of ethanol.

OA-inducing MLI surgery and teriparatide treatment

All experiments involving mice were performed with the approval of the University Committee on Animal Resources at the University of Rochester Medical Center. Ten week-old male C57/BL6 mice were administered meniscal/ligamentous injury (MLI) to the right knee and sham surgery to the left knee using a surgical method that we established previously [38]. Following administration of anesthesia (IP injection of 60 mg/kg ketamine, 4 mg/kg xylazine), a 5 mm-long incision was made on the medial aspect of the joint. With the aid of surgical loops, the medial collateral ligament was transected, the joint space was opened slightly and a 25 gauge needle was used to detach the medial meniscus from its anterior attachment to the tibia. Scissors were then used to remove a portion of the detached meniscus. Sham surgery involved a similar incision to open, but tissues were not manipulated. Following this, the skin was closed with 3–0 silk sutures applied in an interrupted pattern. Post-surgery, mice were provided analgesia (IP injection of 0.5 mg/kg buprenorphine) every 12 h for 72 h and the sutures were removed after 10 days.

Animals began daily subcutaneous injection of sterile 0.9% NaCl (Braun), 40 μg/kg Forteo that was purchased from Eli Lilly, or 40 μg/kg recombinant human parathyroid hormone (1–34) (PTH) that was purchased from Sigma. The daily injections commenced immediately or

8 weeks following surgery and continued until recovery of tissues for analysis. Teriparatide dosage was chosen based on two studies demonstrating that the 30–40 μg/kg/day dose range accelerates fracture healing in the mouse, primarily through enhanced chondrogenesis and expansion of the cartilaginous callus [65, 66].

Murine tissue fixation and histology preparation

A previously established systematic approach to preparation, sectioning and visualizing articular cartilage was employed for all tissue-based assays [38]. At the time of harvest, mice were sacrificed using an AMVA-approved method and the surgically-manipulated knee joints were dissected with the femur and tibia intact to maintain the structural integrity of the joint. Tissues were fixed at room temperature in 10% neutral buffered formalin for 72 h, decalcified in 14% w/v EDTA for 14 days, processed using a microwave processor, and embedded in paraffin. Tissue blocks were then serially sectioned in the midsagittal plane through the medial compartment of the joint. A series of 3 μm-thick sections were cut at three levels within the medial compartment, each level being 50 μm from the previous level. These cut sections were mounted on positively-charged glass slides, baked at 60°C overnight, de-paraffinized in xylene, and rehydrated in decreasing concentrations of ethanol. Some sections were stained with Alcian Blue and Orange G for Chambers scoring and histomorphometry. Unstained sections were used for immunohistochemistry and *in situ* hybridization.

Molecular analysis of tissues

Human and mouse sections evaluated by immunohistochemistry were treated with 3% hydrogen peroxide for 20 min, followed by a 1:20 dilution of normal goat serum for 20 min. Slides were incubated overnight at 4°C with a mouse anti-human PTHR1 monoclonal antibody (1:50; Upstate Cell Signaling), a rabbit anti-mouse JAG1 polyclonal antibody (1:100; Chemicon International), a mouse anti-human MMP13 monoclonal antibody (1:200; Thermo Scientific), a mouse anti-human COL10a1 monoclonal antibody (1:50; Quartett Immunodiagnostika & Biotechnologie), a mouse anti-human c-terminal aggrecan neoepitope NITEGE (1:400; mdbioproducts), or a mouse anti-human RUNX2 monoclonal antibody (1:100, MBL). Following this, slides were rinsed with phosphate-buffered saline (PBS), and incubated for 30 min at room temperature with a biotinylated goat anti-mouse IgG (1:200; Vector; for PTHR1 and COL10a1), goat-anti-rabbit IgG (1:200; Vector; for JAG1), horse anti-mouse/rabbit/goat IgG (1:200; Vector; for MMP13 and NITEGE), or rabbit anti-mouse IgG (1:200; Vector; for RUNX2). Antibody binding to antigen was detected following application of HRP Streptavidin (1:250) with a 5 min application of Romulin AEC Chromagen (Bio care Medical). Nuclei were counterstained for 20 s with Tacha's AEC Chromogen (Bio care Medical). *In situ* hybridization analysis of mouse tissues was performed as described [81, 82] using ^{35}S-labeled riboprobes. The *Col1a1* probe was developed previously [82] and the *Prg4* probe was generated from a plasmid containing a cDNA clone of the gene (Open Biosystems; clone #40140700).

Mouse articular cartilage mRNA isolation and qPCR analysis

Eight weeks following surgery, mice were sacrificed and tibial plateau cartilage from MLI or sham-operated joints was carefully dissected with the aid of surgical loops. Dissected cartilage was immediately frozen on dry ice and stored at −80°C until extraction of total RNA. RNA was isolated from pooled tibial plateau cartilage from 15 joints via homogenization, followed by digestion in TRIzol using the manufacturer's instructions. One μg of total RNA was used to make cDNA using SSII reverse transcriptase (Invitrogen). The abundance of mouse β-actin and various genes of interest was then assessed by qPCR using a Rotor Gene 6000 PCR machine (Corbett Research) using the following primer sets: 5′-TGTTACCAACTGGGACGACA-3′ and 5′-CTGGGTCATCTTTTCACGGT-3′ (*β-actin*);

5′-ACTCCTTCCAGGGATTTTTTGTT-3′ and 5′-GAAGTCCAATGCCAGTGTCCA-3′ (*Pthr1*); 5′-ATCCAGCTAAGACACAGCAAGCCA-3′ and 5′-TGGAGCACAAAGGAGTGGTCTCAA-3′ (*Mmp13*); and 5′-GCTACTGCACAGGGAAGAGG-3′ and 5′-TGCATATTTGGGAACCCATT-3′ (*Adamts5*).

Mouse OARSI scoring of cartilage

Semi-quantitative histopathologic grading was performed using a derivative of the Chambers' scoring system [74, 83] that has been established by the OARSI histopathology initiative as the standard method for grading of mouse cartilage degeneration [84]. Based on this system, cartilage grading was carried out using Alcian Blue/Orange G-stained midsagittal sections using the following scale, where: 0 = normal cartilage, 0.5 = loss of proteoglycan stain without cartilage damage, 1 = mild superficial fibrillation, 2 = fibrillation and/or clefting extending below the superficial zone, 3 = mild (<25%) loss of cartilage, 4 = moderate (25–50%) loss of cartilage, 5 = severe (50–75%) loss of non-calcified cartilage, and 6 = eburnation with >75% loss of cartilage. Grading was performed by three blinded observers (R.N.R., M.J.Z., and E.R.S.). Observer agreement was evaluated in pairs via calculation of a weighted kappa coefficient, using Fleiss-Cohen weights, as we have described [38]. The E.R.S. versus R.N.R. coefficient was 0.94, the E.R.S. versus M.J.Z. coefficient was 0.90, and the R.N.R. versus M.J.Z. coefficient was 0.89, all indicative of strong agreement between the observers. The three grades for each section were averaged and the data from each group of mice was combined.

Histomorphometric determination of cartilage area

A blinded observer (E.R.S.) quantified articular cartilage area via histomorphometry, as previously described [38]. Briefly, using Alcian Blue/Orange G-stained sections, the OsteoMetrics system (OsteoMetrics) was used to quantify articular cartilage area on one tissue section at each of three levels (50 μm apart) in the medial compartment of every joint. Using the OsteoMetrics stylus, projected images of the articular cartilage, obtained using an Olympus microscope (40× objective) outfitted with a video camera, were outlined on the femoral condyle and tibial plateau in an area that was 200 μm wide (centered on the joint). Zones of erosion and calcified cartilage were excluded from outlined area. Then, using an area-calculating algorithm in the Osteomeasure software, the area of collected ROIs was quantified for every section. Area values for every section from a given joint were then averaged.

Quantification of Alcian Blue staining intensity

One representative Alcian Blue/Orange G-stained section from each joint (MLI and sham) of each experimental animal was photographed and analyzed using ImageJ by splitting the color image into its corresponding red, green, and blue channels. The derivative red channel image was then inverted. A threshold of 155 to 255 was selected for all inverted images. Values that fell within this range were taken to be regions of Alcian Blue staining. The grey scales within the selected threshold range were integrated and normalized to the mean integrated intensities of articular cartilage from the saline-treated group.

MicroCT assessment of bone volume

Prior to histologic processing, harvested knee joints were evaluated via microCT using a Scanco vivaCT40 scanner with a 55 kVp source as we have previously described [38]. Joints were scanned at a resolution of 12 μm with a slice increment of 10 μm from mid-femur to mid-tibia. Images from each group were reconstructed at identical thresholds to allow 3D

structural rendering of each joint. Histomorphometric analysis of bone volume was performed on selected regions between the femoral and tibial physes.

Quantification of osteophytes

Osteophyte number and diameter were assessed by a blinded observer (E.R.S.) on projected 40× images of Alcian Blue/Orange G-stained sections from each of three levels (50 μm apart) in the medial compartment of every joint. Osteophytes at both the anterior and posterior margins were included in assessments. Using methods reported in Janusz *et al.* [77], the mean osteophyte diameter (measured in two dimensions) was determined using a graticule with 100 μm increments.

Statistical analyses

For all qPCR analyses, Mouse OARSI scoring, quantification of Alcian Blue staining and cartilage area determinations, statistically significant differences were identified by unpaired, two-tailed Student's *t* tests, with *p*-values <0.05 denoting significance. For microCT-based quantification of bone volume, statistically significant differences were identified by ANOVA, again with *P* values < 0.05 denoting significance. All error bars represent SEM except in the microCT analyses where the whiskers represent the value of the maximum and minimum data point in the set.

Supplementary Material

Refer to Web version on PubMed Central for supplementary material.

Acknowledgments

The authors wish to thank E. Dussmann, R. Maynard, N. Miller and N. Alcock for excellent technical assistance and M. Thullen for performing microCT analyses. We also wish to thank C. Beck in the Biostatistics Department at the University of Rochester Medical Center for advice and help with statistical analysis of raw data. For processing and sectioning of tissue samples, as well as for performing immunohistochemistry and in situ hybridization, we thank R. Tierney, S. Mack, A. Mirando, N. Porecha, and A. Thomas of the Histology, Biochemistry, and Molecular Imaging (HBMI) Core in the Center for Musculoskeletal Research.

Funding: This work was supported by NIH/NIAMS P50 AR054041 (R.N.R.), NIH/NIAMS R01 AR045700 (R.N.R.), and an Arthritis Foundation Arthritis Investigator Award (M.J.Z). E.R.S. was supported by NIH/NIAMS T32 AR053459 (M.J.Z.).

REFERENCES AND NOTES

1. CDC, Prevalence and most common causes of disability among adults--United States 2005. MMWR Morb Mortal Wkly Rep. 2009; 58:421–426. [PubMed: 19407734]
2. Helmick CG, Felson DT, Lawrence RC, Gabriel S, Hirsch R, Kwoh CK, Liang MH, Kremers HM, Mayes MD, Merkel PA, Pillemer SR, Reveille JD, Stone JH. Estimates of the prevalence of arthritis and other rheumatic conditions in the United States. Part I 2. Arthritis and Rheumatism. 2008; 58:15–25. [PubMed: 18163481]
3. Hootman JM, Helmick CG. Projections of US prevalence of arthritis and associated activity limitations 5. Arthritis and Rheumatism. 2006; 54:226–229. [PubMed: 16385518]
4. Felson DT. Clinical practice. Osteoarthritis of the knee. N Engl J Med. 2006; 354:841–848. [PubMed: 16495396]
5. Samuels J, Krasnokutsky S, Abramson SB. Osteoarthritis: a tale of three tissues. Bull NYU Hosp Jt Dis. 2008; 66:244–250. [PubMed: 18937640]
6. Sellam J, Berenbaum F. The role of synovitis in pathophysiology and clinical symptoms of osteoarthritis. Nat Rev Rheumatol. 2010; 6:625–635. [PubMed: 20924410]
7. Englund M. The role of biomechanics in the initiation and progression of OA of the knee 9. Best Pract Res Clin Rheumatol. 2010; 24:39–46. [PubMed: 20129198]

8. Roos H, Lauren M, Adalberth T, Roos EM, Jonsson K, Lohmander LS. Knee osteoarthritis after meniscectomy: prevalence of radiographic changes after twenty-one years, compared with matched controls 2. Arthritis and Rheumatism. 1998; 41:687–693. [PubMed: 9550478]
9. Thomas A, Eichenberger G, Kempton C, Pape D, York S, Decker AM, Kohia M. Recommendations for the treatment of knee osteoarthritis, using various therapy techniques, based on categorizations of a literature review 1. J Geriatr Phys Ther. 2009; 32:33–38. [PubMed: 19856634]
10. Pacifici M, Koyama E, Shibukawa Y, Wu C, Tamamura Y, Enomoto-Iwamoto M, Iwamoto M. Cellular and molecular mechanisms of synovial joint and articular cartilage formation. Ann N Y Acad Sci. 2006; 1068:74–86. [PubMed: 16831907]
11. Buckwalter JA, Mankin HJ. Articular cartilage. Journal of Bone and Joint Surgery. 1997; 79A: 600–632.
12. Aigner T, Reichenberger E, Bertling W, Kirsch T, Stoss H, von der MK. Type × collagen expression in osteoarthritic and rheumatoid articular cartilage. Virchows ArchB Cell Pathol Incl Mol Pathol. 1993; 63:205–211.
13. Aigner T, Gluckert K, von der Mark K. Activation of fibrillar collagen synthesis and phenotypic modulation of chondrocytes in early human osteoarthritic cartilage lesions. Osteoarthritis and Cartilage. 1997; 5:183–189. [PubMed: 9219681]
14. Aigner T, Kim HA, Roach HI. Apoptosis in osteoarthritis. Rheum Dis Clin North Am. 2004; 30:639–653. xi. [PubMed: 15261346]
15. Aigner T, Soder S, Gebhard PM, McAlinden A, Haag J. Mechanisms of disease: role of chondrocytes in the pathogenesis of osteoarthritis--structure, chaos and senescence. Nat Clin Pract Rheumatol. 2007; 3:391–399. [PubMed: 17599073]
16. Jilka RL, Weinstein RS, Bellido T, Roberson P, Parfitt AM, Manolagas SC. Increased bone formation by prevention of osteoblast apoptosis with parathyroid hormone. J Clin Invest. 1999; 104:439–446. [PubMed: 10449436]
17. Compston JE. Skeletal actions of intermittent parathyroid hormone: effects on bone remodelling and structure. Bone. 2007; 40:1447–1452. [PubMed: 17045858]
18. Compston J. Does parathyroid hormone treatment affect fracture risk or bone mineral density in patients with osteoporosis? Nat Clin Pract Rheumatol. 2007; 3:324–325. [PubMed: 17471283]
19. FDA, Forteo approved for osteoporosis treatment. FDA Consum. 2003; 37:4.
20. Schnoke M, Midura SB, Midura RJ. Parathyroid hormone suppresses osteoblast apoptosis by augmenting DNA repair. Bone. 2009; 45:590–602. [PubMed: 19450716]
21. Pettway GJ, Meganck JA, Koh AJ, Keller ET, Goldstein SA, McCauley LK. Parathyroid hormone mediates bone growth through the regulation of osteoblast proliferation and differentiation. Bone. 2008; 42:806–818. [PubMed: 18234576]
22. Kronenberg HM, Karaplis AC, Lanske B. Role of parathyroid hormone-related protein in skeletal development. Annals of the New York Academy of Sciences. 1996; 785:119–123. [PubMed: 8702116]
23. Kronenberg HM. PTHrP and skeletal development. Annals of the New York Academy of Sciences. 2006; 1068:1–13. [PubMed: 16831900]
24. Adams SL, Cohen AJ, Lassova L. Integration of signaling pathways regulating chondrocyte differentiation during endochondral bone formation. JCell Physiol. 2007; 213:635–641. [PubMed: 17886256]
25. Burdan F, Szumilo J, Korobowicz A, Farooquee R, Patel S, Patel A, Dave A, Szumilo M, Solecki M, Klepacz R, Dudka J. Morphology and physiology of the epiphyseal growth plate. Folia Histochem Cytobiol. 2009; 47:5–16. [PubMed: 19419931]
26. Karaplis AC, Luz A, Glowacki J, Bronson RT, Tybulewicz VL, Kronenberg HM, Mulligan RC. Lethal skeletal dysplasia from targeted disruption of the parathyroid hormone-related peptide gene. Genes and Development. 1994; 8:277–289. [PubMed: 8314082]
27. Lanske B, Karaplis AC, Lee K, Luz A, Vortkamp A, Pirro A, Karperien M, Defize LHK, Ho C, Mulligan RC, Abou-Samra AB, Juppner H, Segre GV, Kronenberg HM. PTH/PTHrP receptor in early development and Indian hedgehog-regulated bone growth. Science. 1996; 273:663–666. [PubMed: 8662561]

28. Weir EC, Philbrick WM, Amling M, Neff LA, Baron R, Broadus AE. Targeted overexpression of parathyroid hormone-related peptide in chondrocytes causes chondrodysplasia and delayed endochondral bone formation. Proceedings of the National Academy of Sciences USA. 1996; 93:10240–10245.
29. Schipani E, Lanske B, Hunzelman J, Luz A, Kovacs CS, Lee K, Pirro A, Kronenberg HM, Juppner H. Targeted expression of constitutively active receptors for parathyroid hormone and parathyroid hormone-related peptide delays endochondral bone formation and rescues mice that lack parathyroid hormone-related peptide. Proceedings of the National Academy of Sciences USA. 1997; 94:13689–13694.
30. Schipani E, Provot S. PTHrP, PTH, and the PTH/PTHrP receptor in endochondral bone development. Birth Defects Res C Embryo Today. 2003; 69:352–362. [PubMed: 14745975]
31. Provot S, Schipani E. Molecular mechanisms of endochondral bone development. Biochemical and Biophysical Research Communications. 2005; 328:658–665. [PubMed: 15694399]
32. Broadus AE, Macica C, Chen X. The PTHrP functional domain is at the gates of endochondral bones. Ann N Y Acad Sci. 2007; 1116:65–81. [PubMed: 18083922]
33. Chen X, Macica CM, Nasiri A, Broadus AE. Regulation of articular chondrocyte proliferation and differentiation by indian hedgehog and parathyroid hormone-related protein in mice. Arthritis and Rheumatism. 2008; 58:3788–3797. [PubMed: 19035497]
34. Godler DE, Stein AN, Bakharevski O, Lindsay MM, Ryan PF. Parathyroid hormone-related peptide expression in rat collagen-induced arthritis. Rheumatology(Oxford). 2005; 44:1122–1131. [PubMed: 15901905]
35. Macica C, Liang G, Nasiri A, Broadus AE. Genetic evidence that parathyroid hormone-related protein regulates articular chondrocyte maintenance. Arthritis Rheum. 2011
36. Terkeltaub R, Lotz M, Johnson K, Deng D, Hashimoto S, Goldring MB, Burton D, Deftos LJ. Parathyroid hormone-related proteins is abundant in osteoarthritic cartilage, and the parathyroid hormone-related protein 1–173 isoform is selectively induced by transforming growth factor beta in articular chondrocytes and suppresses generation of extracellular inorganic pyrophosphate. Arthritis and Rheumatism. 1998; 41:2152–2164. [PubMed: 9870872]
37. Kamekura S, Hoshi K, Shimoaka T, Chung U, Chikuda H, Yamada T, Uchida M, Ogata N, Seichi A, Nakamura K, Kawaguchi H. Osteoarthritis development in novel experimental mouse models induced by knee joint instability. Osteoarthritis Cartilage. 2005; 13:632–641. [PubMed: 15896985]
38. Sampson ER, Beck CA, Ketz J, Canary KL, Hilton MJ, Awad H, Schwarz EM, Chen D, O'Keefe RJ, Rosier RN, Zuscik MJ. Establishment of an index with increased sensitivity for assessing murine arthritis. J Orthop Res. 2011
39. Wright AA, Cook C, Abbott JH. Variables associated with the progression of hip osteoarthritis: a systematic review. Arthritis Rheum. 2009; 61:925–936. [PubMed: 19565541]
40. Weber JM, Forsythe SR, Christianson CA, Frisch BJ, Gigliotti BJ, Jordan CT, Milner LA, Guzman ML, Calvi LM. Parathyroid hormone stimulates expression of the Notch ligand Jagged1 in osteoblastic cells. Bone. 2006; 39:485–493. [PubMed: 16647886]
41. Rhee DK, Marcelino J, Baker M, Gong Y, Smits P, Lefebvre V, Jay GD, Stewart M, Wang H, Warman ML, Carpten JD. The secreted glycoprotein lubricin protects cartilage surfaces and inhibits synovial cell overgrowth. J Clin Invest. 2005; 115:622–631. [PubMed: 15719068]
42. Rhee DK, Marcelino J, Al-Mayouf S, Schelling DK, Bartels CF, Cui Y, Laxer R, Goldbach-Mansky R, Warman ML. Consequences of disease-causing mutations on lubricin protein synthesis, secretion, and post-translational processing. J Biol Chem. 2005; 280:31325–31332. [PubMed: 16000300]
43. Buckwalter JA, Mankin HJ, Grodzinsky AJ. Articular cartilage and osteoarthritis. Instr Course Lect. 2005; 54:465–480. [PubMed: 15952258]
44. Vangsness CT Jr, Spiker W, Erickson J. A review of evidence-based medicine for glucosamine and chondroitin sulfate use in knee osteoarthritis. Arthroscopy. 2009; 25:86–94. [PubMed: 19111223]
45. Zhang W, Nuki G, Moskowitz RW, Abramson S, Altman RD, Arden NK, Bierma-Zeinstra S, Brandt KD, Croft P, Doherty M, Dougados M, Hochberg M, Hunter DJ, Kwoh K, Lohmander LS, Tugwell P. OARSI recommendations for the management of hip and knee osteoarthritis: part III:

Changes in evidence following systematic cumulative update of research published through January 2009. Osteoarthritis Cartilage. 2010; 18:476–499. [PubMed: 20170770]

46. Brzusek D, Petron D. Treating knee osteoarthritis with intra-articular hyaluronans. Curr Med Res Opin. 2008; 24:3307–3322. [PubMed: 18954498]
47. Brander VA, Stadler TS. Functional improvement with hylan G-F 20 in patients with knee osteoarthritis. Phys Sportsmed. 2009; 37:38–48. [PubMed: 20048527]
48. Kamekura S, Kawasaki Y, Hoshi K, Shimoaka T, Chikuda H, Maruyama Z, Komori T, Sato S, Takeda S, Karsenty G, Nakamura K, Chung UI, Kawaguchi H. Contribution of runt-related transcription factor 2 to the pathogenesis of osteoarthritis in mice after induction of knee joint instability. Arthritis and Rheumatism. 2006; 54:2462–2470. [PubMed: 16868966]
49. Buckwalter JA, Brown TD. Joint injury, repair, and remodeling: roles in post-traumatic osteoarthritis. Clin Orthop Relat Res. 2004:7–16. [PubMed: 15232420]
50. Yang X, Chen L, Xu X, Li C, Huang C, Deng CX. TGF-beta/Smad3 signals repress chondrocyte hypertrophic differentiation and are required for maintaining articular cartilage. Journal of Cell Biology. 2001; 153:35–46. [PubMed: 11285272]
51. Serra R, Johnson M, Filvaroff EH, LaBorde J, Sheehan DM, Derynck R, Moses HL. Expression of truncated. kinase-defective TGF-beta type II receptor in mouse skeletal muscle promotes terminal chondrocyte differentiation and osteoarthritis. Journal of Cell Biology. 1997; 139:541–552. [PubMed: 9334355]
52. Wu Q, Kim KO, Sampson ER, Chen D, Awad H, O'Brien T, Puzas JE, Drissi H, Schwarz EM, O'Keefe RJ, Zuscik MJ, Rosier RN. Induction of an osteoarthritis-like phenotype and degradation of phosphorylated Smad3 by Smurf2 in transgenic mice. Arthritis and Rheumatism. 2008; 58:3132–3144. [PubMed: 18821706]
53. Zhu M, Tang D, Wu Q, Hao S, Chen M, Xie C, Rosier RN, O'Keefe RJ, Zuscik M, Chen D. Activation of beta-catenin signaling in articular chondrocytes leads to osteoarthritis-like phenotype in adult beta-catenin conditional activation mice. Journal of Bone and Mineral Research. 2009; 24:12–21. [PubMed: 18767925]
54. Wu Q, Huang JH, Sampson ER, Kim KO, Zuscik MJ, O'Keefe RJ, Chen D, Rosier RN. Smurf2 induces degradation of GSK-3beta and upregulates beta-catenin in chondrocytes: a potential mechanism for Smurf2-induced degeneration of articular cartilage. Experimental Cell Research. 2009; 315:2386–2398. [PubMed: 19481076]
55. Loughlin J, Dowling B, Chapman K, Marcelline L, Mustafa Z, Southam L, Ferreira A, Ciesielski C, Carson DA, Corr M. Functional variants within the secreted frizzled-related protein 3 gene are associated with hip osteoarthritis in females. Proc Natl Acad Sci USA. 2004; 101:9757–9762. [PubMed: 15210948]
56. Min JL, Meulenbelt I, Riyazi N, Kloppenburg M, Houwing-Duistermaat JJ, Seymour AB, Pols HA, van Duijn CM, Slagboom PE. Association of the Frizzled-related protein gene with symptomatic osteoarthritis at multiple sites. Arthritis and Rheumatism. 2005; 52:1077–1080. [PubMed: 15818669]
57. Lane NE, Lian K, Nevitt MC, Zmuda JM, Lui L, Li J, Wang J, Fontecha M, Umblas N, Rosenbach M, de Leon P, Corr M. Frizzled-related protein variants are risk factors for hip osteoarthritis. Arthritis Rheum. 2006; 54:1246–1254. [PubMed: 16572458]
58. Lin AC, Seeto BL, Bartoszko JM, Khoury MA, Whetstone H, Ho L, Hsu C, Ali SA, Alman BA. Modulating hedgehog signaling can attenuate the severity of osteoarthritis. Nat Med. 2009; 15:1421–1425. [PubMed: 19915594]
59. Saito T, Fukai A, Mabuchi A, Ikeda T, Yano F, Ohba S, Nishida N, Akune T, Yoshimura N, Nakagawa T, Nakamura K, Tokunaga K, Chung UI, Kawaguchi H. Transcriptional regulation of endochondral ossification by HIF-2alpha during skeletal growth and osteoarthritis development. Nat Med. 2010; 16:678–686. [PubMed: 20495570]
60. Yang S, Kim J, Ryu JH, Oh H, Chun CH, Kim BJ, Min BH, Chun JS. Hypoxia-inducible factor-2alpha is a catabolic regulator of osteoarthritic cartilage destruction. Nat Med. 2010; 16:687–693. [PubMed: 20495569]
61. Kawaguchi H. Endochondral ossification signals in cartilage degradation during osteoarthritis progression in experimental mouse models. Mol Cells. 2008; 25:1–6. [PubMed: 18319608]

62. Flannery CR. Novel therapies in OA. Curr Drug Targets. 2010; 11:614–619. [PubMed: 20199389]
63. Chang JK, Chang LH, Hung SH, Wu SC, Lee HY, Lin YS, Chen CH, Fu YC, Wang GJ, Ho ML. Parathyroid hormone 1–34 inhibits terminal differentiation of human articular chondrocytes and osteoarthritis progression in rats 1. Arthritis and Rheumatism. 2009; 60:3049–3060. [PubMed: 19790062]
64. Kudo S, Mizuta H, Takagi K, Hiraki Y. Cartilaginous repair of full-thickness articular cartilage defects is induced by the intermittent activation of PTH/PTHrP signaling. Osteoarthritis Cartilage. 2011; 19:886–894. [PubMed: 21571083]
65. Kakar S, Einhorn TA, Vora S, Miara LJ, Hon G, Wigner NA, Toben D, Jacobsen KA, Al-Sebaei MO, Song M, Trackman PC, Morgan EF, Gerstenfeld LC, Barnes GL. Enhanced chondrogenesis and Wnt signaling in PTH-treated fractures. J Bone Miner Res. 2007; 22:1903–1912. [PubMed: 17680724]
66. Kaback LA, Soung dY, Naik A, Geneau G, Schwarz EM, Rosier RN, O'Keefe RJ, Drissi H. Teriparatide (1–34 human PTH) regulation of osterix during fracture repair. JCell Biochem. 2008; 105:219–226. [PubMed: 18494002]
67. Iida-Klein A, Hughes C, Lu SS, Moreno A, Shen V, Dempster DW, Cosman F, Lindsay R. Effects of cyclic versus daily hPTH(1–34) regimens on bone strength in association with BMD, biochemical markers, and bone structure in mice. J Bone Miner Res. 2006; 21:274–282. [PubMed: 16418783]
68. Alexander JM, Bab I, Fish S, Muller R, Uchiyama T, Gronowicz G, Nahounou M, Zhao Q, White DW, Chorev M, Gazit D, Rosenblatt M. Human parathyroid hormone 1–34 reverses bone loss in ovariectomized mice. J Bone Miner Res. 2001; 16:1665–1673. [PubMed: 11547836]
69. Montero M, Serfati D, Luna S, Diaz-Curiel M, Carrascal MT, Gomez S, De la Piedra C. The effectiveness of intermittent rat parathyroid hormone (1–34) treatment on low bone mass due to oestrogen or androgen depletion in skeletally mature rats. Aging Male. 2010; 13:59–73. [PubMed: 20148746]
70. Nakazawa T, Nakajima A, Shiomi K, Moriya H, Einhorn TA, Yamazaki M. Effects of low-dose, intermittent treatment with recombinant human parathyroid hormone (1–34) on chondrogenesis in a model of experimental fracture healing. Bone. 2005; 37:711–719. [PubMed: 16143574]
71. Mashiba T, Burr DB, Turner CH, Sato M, Cain RL, Hock JM. Effects of human parathyroid hormone (1–34), LY333334, on bone mass, remodeling, and mechanical properties of cortical bone during the first remodeling cycle in rabbits. Bone. 2001; 28:538–547. [PubMed: 11344054]
72. Vahle JL, Zuehlke U, Schmidt A, Westmore M, Chen P, Sato M. Lack of bone neoplasms and persistence of bone efficacy in cynomolgus macaques after long-term treatment with teriparatide [rhPTH(1–34)]. J Bone Miner Res. 2008; 23:2033–2039. [PubMed: 18684088]
73. Subbiah V, Madsen VS, Raymond AK, Benjamin RS, Ludwig JA. Of mice and men: divergent risks of teriparatide-induced osteosarcoma. Osteoporos Int. 2010; 21:1041–1045. [PubMed: 19597911]
74. Glasson SS, Askew R, Sheppard B, Carito B, Blanchet T, Ma HL, Flannery CR, Peluso D, Kanki K, Yang Z, Majumdar MK, Morris EA. Deletion of active ADAMTS5 prevents cartilage degradation in a murine model of osteoarthritis. Nature. 2005; 434:644–648. [PubMed: 15800624]
75. Little CB, Barai A, Burkhardt D, Smith SM, Fosang AJ, Werb Z, Shah M, Thompson EW. Matrix metalloproteinase 13-deficient mice are resistant to osteoarthritic cartilage erosion but not chondrocyte hypertrophy or osteophyte development. Arthritis Rheum. 2009; 60:3723–3733. [PubMed: 19950295]
76. Chockalingam PS, Sun W, Rivera-Bermudez MA, Zeng W, Dufield DR, Larsson S, Lohmander LS, Flannery CR, Glasson SS, Georgiadis KE, Morris EA. Elevated aggrecanase activity in a rat model of joint injury is attenuated by an aggrecanase specific inhibitor. Osteoarthritis Cartilage. 2011; 19:315–323. [PubMed: 21163358]
77. Janusz MJ, Bendele AM, Brown KK, Taiwo YO, Hsieh L, Heitmeyer SA. Induction of osteoarthritis in the rat by surgical tear of the meniscus: Inhibition of joint damage by a matrix metalloproteinase inhibitor. Osteoarthritis Cartilage. 2002; 10:785–791. [PubMed: 12359164]

78. Mapp PI, Walsh DA, Bowyer J, Maciewicz RA. Effects of a metalloproteinase inhibitor on osteochondral angiogenesis, chondropathy and pain behavior in a rat model of osteoarthritis. Osteoarthritis Cartilage. 2010; 18:593–600. [PubMed: 20067755]

79. Tashjian AH Jr, Goltzman D. On the interpretation of rat carcinogenicity studies for human PTH(1–34) and human PTH(1–84). J Bone Miner Res. 2008; 23:803–811. [PubMed: 18435577]

80. Tzioupis CC, Giannoudis PV. The Safety and Efficacy of Parathyroid Hormone (PTH) as a Biological Response Modifier for the Enhancement of Bone Regeneration. Curr Drug Saf. 2006; 1:189–203. [PubMed: 18690930]

81. Long F, Zhang XM, Karp S, Yang Y, McMahon AP. Genetic manipulation of hedgehog signaling in the endochondral skeleton reveals a direct role in the regulation of chondrocyte proliferation. Development. 2001; 128:5099–5108. [PubMed: 11748145]

82. Hilton MJ, Tu X, Wu X, Bai S, Zhao H, Kobayashi T, Kronenberg HM, Teitelbaum SL, Ross FP, Kopan R, Long F. Notch signaling maintains bone marrow mesenchymal progenitors by suppressing osteoblast differentiation 10. Nat Med. 2008; 14:306–314. [PubMed: 18297083]

83. Chambers MG, Cox L, Chong L, Suri N, Cover P, Bayliss MT, Mason RM. Matrix metalloproteinases and aggrecanases cleave aggrecan in different zones of normal cartilage but colocalize in the development of osteoarthritic lesions in STR/ort mice. Arthritis and Rheumatism. 2001; 44:1455–1465. [PubMed: 11407708]

84. Glasson SS, Chambers MG, Van Den Berg WB, Little CB. The OARSI histopathology initiative - recommendations for histological assessments of osteoarthritis in the mouse. Osteoarthritis Cartilage. 2010; 18(Suppl 3):S17–23. [PubMed: 20864019]

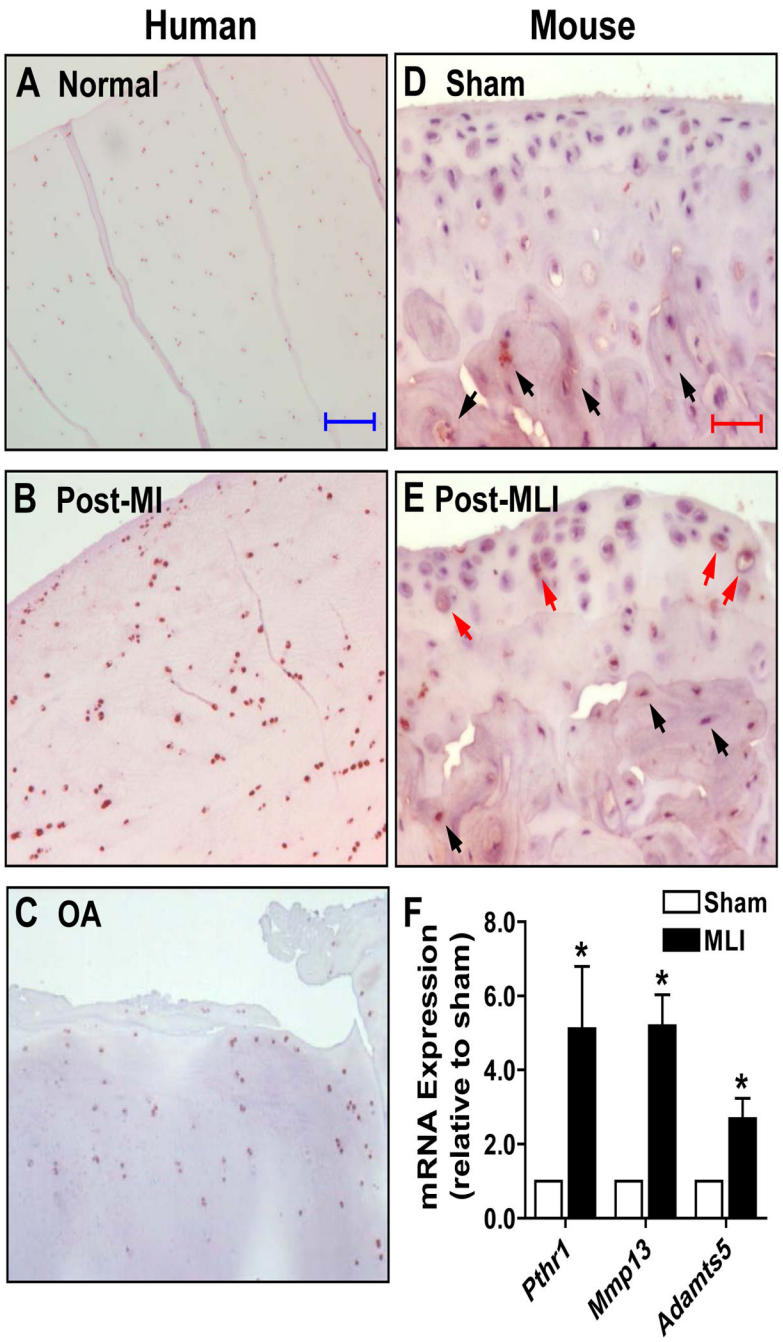

Fig. 1. PTHR1 is increased in human and murine articular cartilage following injury and during OA

(**A** to **C**) Staining for PTHR1 in articular chondrocytes in normal human cartilage (A), cartilage from patients who underwent arthroscopic surgery for a meniscal injury (B), and within OA cartilage from patients who underwent total knee arthroplasty (C). Blue scale bar in Panel A = 100 μm and is applicable to panels A thru C. (**D** and **E**) PTHR1 expression in articular chondrocytes within sham-operated, uninjured mouse knee cartilage (D) and arthritic cartilage from mice with MLI injury (E, red arrows). Osteoblasts and osteocytes in the subchondral plate positive for PTHR1 are indicated by black arrows. Red scale bar in D = 25 μm and is applicable to panels D and E. (**F**) qPCR analysis of mRNA of chondrocytic

markers isolated from the tibial plateau articular cartilage of mice that underwent sham and MLI surgery. *$P < 0.05$ compared to respective sham controls using an unpaired, two-tailed Student's *t* test, bars represent means +/− SEM, $n=3$.

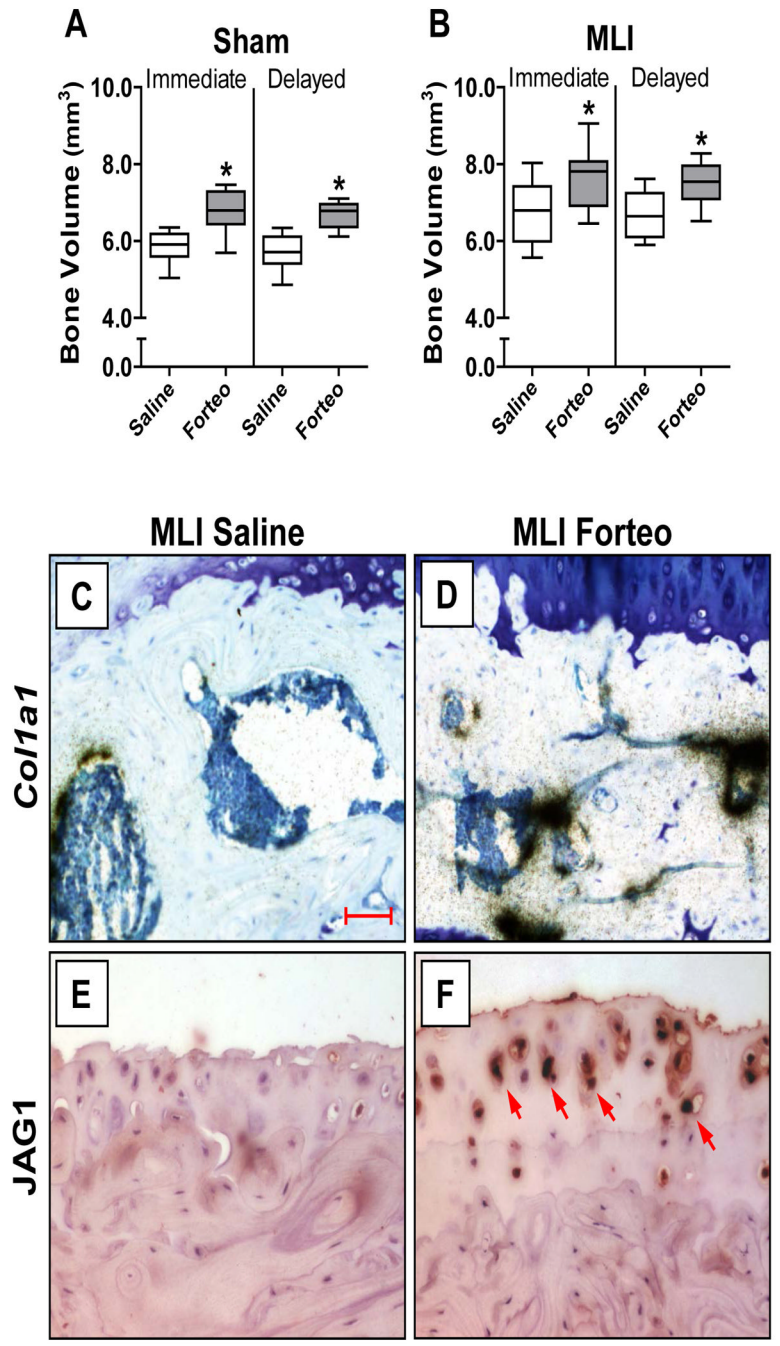

Fig. 2. Systemic Forteo treatment has a bone anabolic effect and induces articular chondrocyte up-regulation of JAG1 in MLI joints

(**A** and **B**) MicroCT scans were performed on sham-operated and MLI mouse joints 12 weeks post-surgery, and bone volume in the region between the physes was quantified. The median bone volume for each experimental group is indicated by the horizontal line within each box plot, with the top and bottom of each box indicating the 75th and 25th percentile, respectively, n=10. Whiskers denote maximum and minimum data points in the set. *P < 0.05 compared to respective sham controls using ANOVA. (**C** to **F**) Eight weeks after sham or MLI surgery, either saline or Forteo was administered to the mice daily for 4 weeks (delayed administration). Representative sections are shown hybridized with a probe specific

for *Col1a1* in the subchondral bone of MLI joints from Forteo-treated mice (D) and saline-treated mice (C). Representative unstained sections from these same joints were also probed with a JAG1 antibody to reveal immunoreactivity in articular chondrocytes (red arrows) (E, F). Red scale bar in panel C = 25 μm and is applicable to panels C thru F.

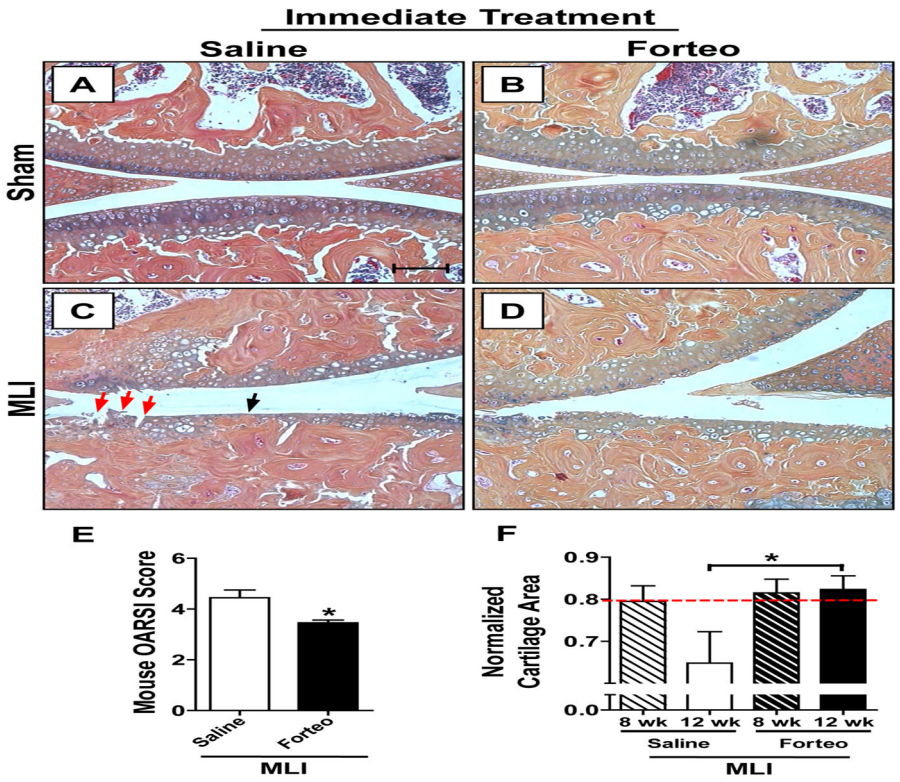

Fig. 3. Immediate treatment with Forteo protects against articular cartilage degeneration in MLI joints

Mice underwent MLI (right knee) and sham (left knee) surgery and then immediately began daily systemic saline or Forteo treatment for 12 weeks. (**A** to **D**) Representative Alcian Blue/Orange G staining for cartilage degeneration following MLI or sham surgery in immediate saline-treated (A, C) and immediate Forteo-treated (B, D) animals. In (C), red arrows identify areas of fibrillation and clefting and the black arrow identifies eburnation (erosion to subchondral bone). Black scale bar in panel A = 50 μm and is applicable to panels A thru D. (**E** and **F**) Chondro-protective effects of immediate Forteo treatment were confirmed by Mouse OARSI scoring (E) and by cartilage area determination (F). **P* < 0.05 compared to respective saline-treated MLI or sham controls using an unpaired, two-tailed Student's *t* test. Bars represent mean +/− SEM. The white hatched bar and red line indicates the average normalized cartilage area in joints 8 weeks following MLI in saline-treated animals.

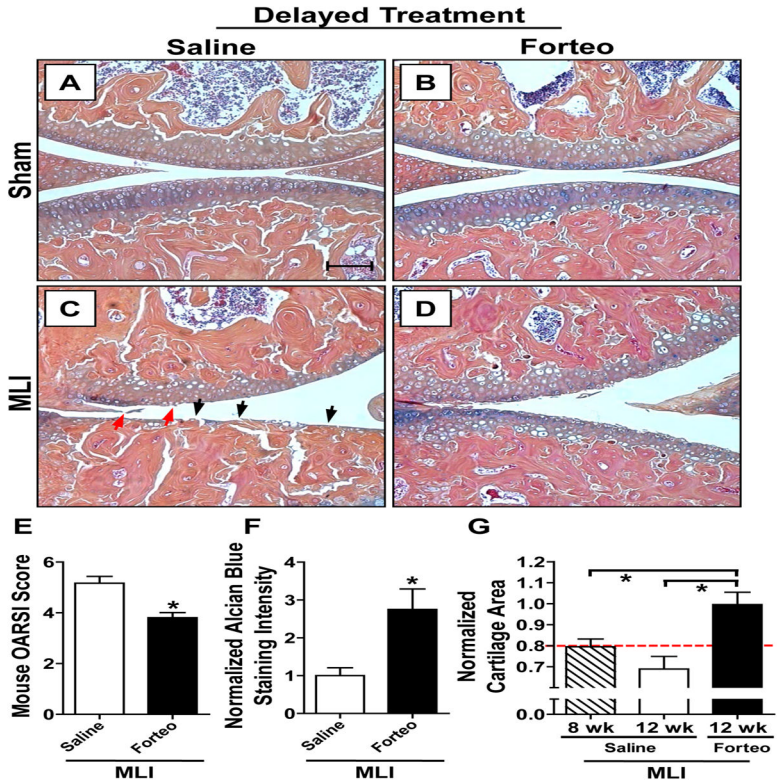

Fig. 4. Delayed Forteo treatment induces chondro-regeneration in MLI joints

Eight weeks after MLI or sham surgery, mice began receiving daily systemic saline or Forteo treatment for 4 weeks. Joints were collected at week 12 for histological analysis. (**A** to **D**) Representative Alcian Blue/Orange G staining for cartilage degeneration following MLI or sham surgery in delayed saline-treated (A, C) and delayed Forteo-treated (B, D) animals. In (C), red arrows identify areas of fibrillation and clefting and black arrows identify areas of cartilage erosion and eburnation. Black scale bar in panel A = 50 μm and is applicable to panels A thru D. (**E** to **G**) Mouse OARSI score (E), Alcian Blue staining normalized to the sham control group (F) and cartilage area histomorphometry normalized to the sham control group (G) collectively establish effects of Forteo on cartilage integrity. **P* < 0.05 compared to respective sham controls using an unpaired, two-tailed Student's *t* test. Bars represent means +/− SEM, *n*=5.

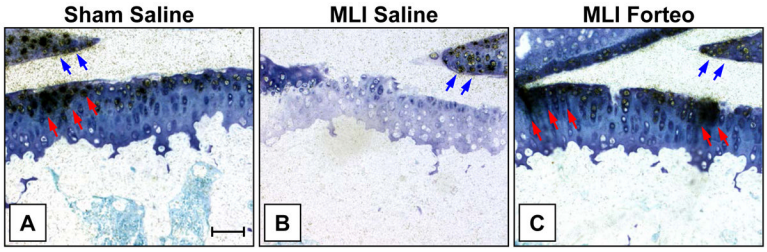

Fig. 5. Delayed Forteo treatment induces articular chondrocyte Prg4 expression in MLI joints

(**A** to **C**) *Prg4* expression (red arrows) in articular chondrocytes from sham-operated (A) and MLI joints (B, C), assessed via in situ hybridization in sections cut from the same experimental groups depicted in Fig. 4 (delayed Forteo treatment). Black arrows identify areas of *Prg4* expression in menisci. Black scale bar in panel A = 50 μm and is applicable to all panels.

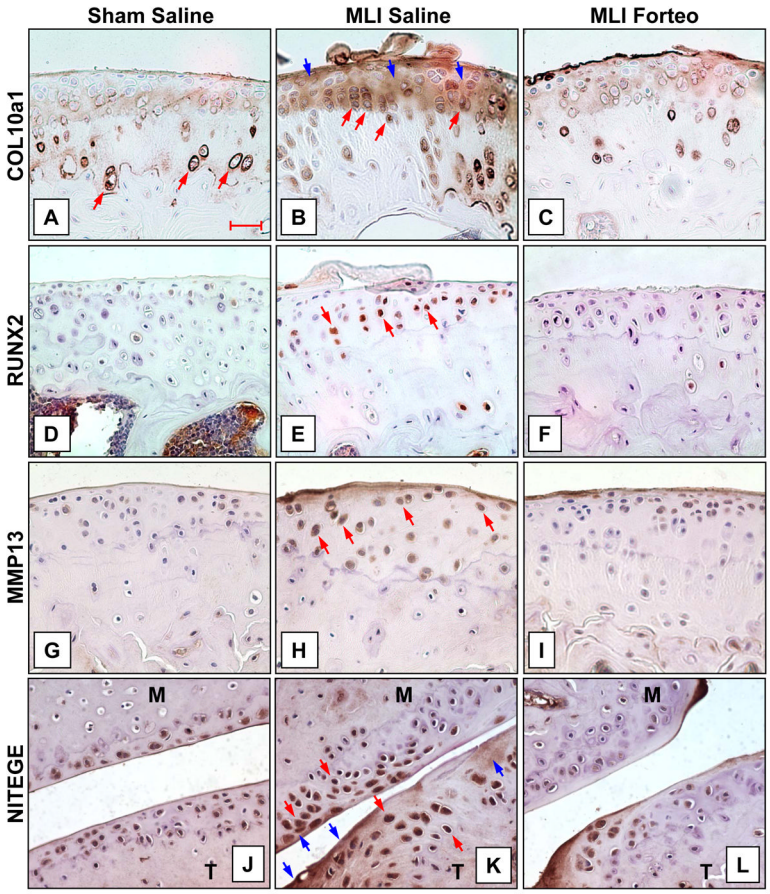

Fig. 6. Forteo inhibits chondrocyte maturation and reduces MMP-13 levels in MLI joints

(**A** to **F**) Immunohistochemistry of cellular/matrix COL10a1 (A to C) and cellular RUNX2 (D to F) protein levels in MLI joints and sham controls. Red arrows indicate cellular staining and blue arrows indicate matrix staining. (**G** to **I**) Articular chondrocyte expression of MMP13 in MLI joints (H, I) and sham controls (G). (**J** to **L**) Immunhistochemical detection of the aggrecan cleavage product containing the C-terminal neoepitope NITEGE in matrix (blue arrows) and cells (red arrows) in the meniscus (M) and tibial plateau articular cartilage (T) from MLI joints (K, L) and sham controls (J). Red scale bar in panel A = 25 μm and is applicable to all panels.